*muscles*

MDPI

*Article*

# Shoulder Biomechanical and Morphological Characteristics Across Para-Swimming Functional Classes: A Comparative Ultrasound Study

**Beata Pożarowszczyk-Kuczko [1], Gabriela Lampart [2], Robert Trybulski [3,4], Maciej Kentel [5] and Sebastian Klich [1,*]**

[1] Department of Sport Didactics, Wrocław University of Health and Sport Science, 51-612 Wrocław, Poland; beata.pozarowszczyk-kuczko@awf.wroc.pl
[2] Doctoral School of Medical and Health Sciences, Medical College, Jagiellonian University, 31-008 Kraków, Poland; gabriela.lampart@doctoral.uj.edu.pl
[3] Department of Medical Sciences, The Wojciech Korfanty Upper Silesian Academy, 40-659 Katowice, Poland; rtrybulski.provita@gmail.com
[4] Provita Żory Medical Center, 44-240 Żory, Poland
[5] eMKaMED Medical Center, 53-110 Wrocław, Poland; emkamed.cm@gmail.com
* Correspondence: sebastian.klich@awf.wroc.pl

**Abstract**

The purpose of this study was to compare dominant-shoulder functional performance and ultrasonographic characteristics between para swimmers classified as S1–S6 and S7–S10. This cross-sectional study included 40 elite para swimmers, comprising 20 manual wheelchair users in the S1–S6 group and 20 ambulatory athletes in the S7–S10 group. Standardized testing on the dominant shoulder evaluated isometric strength and rate of force development (RFD), active range of motion (ROM), supraspinatus tendon (SST) thickness, occupation ratio, ultrasound image texture (PSFR), and acromiohumeral distance (AHD) at 0°, 60°, and 90° abduction. The HL swimmers demonstrated significantly higher pull peak force (219.40 ± 30.78 N vs. 100.30 ± 7.06 N, $p < 0.001$, d = −5.33), abduction peak force (163.00 ± 32.96 N vs. 93.70 ± 7.53 N, $p < 0.001$, d = −2.90), pull RFD (595.05 ± 118.37 N/s vs. 222.10 ± 44.00 N/s, $p < 0.001$), and active ROM (flexion: 173.60 ± 4.65° vs. 142.45 ± 28.48°, $p < 0.001$; abduction: 166.85 ± 4.06° vs. 150.95 ± 22.86°, $p = 0.001$). Conversely, LL swimmers exhibited significantly thicker SST (5.93 ± 0.54 mm vs. 4.89 ± 0.49 mm, $p < 0.001$, d = 2.02), higher occupation ratio (62.70 ± 6.17% vs. 51.10 ± 5.46%, $p < 0.001$, d = 1.99), elevated PSFR (2.21 ± 0.25 $mm^{-1}$ vs. 1.42 ± 0.28 $mm^{-1}$, $p < 0.001$, d = 2.98), and a different angle-dependent AHD pattern (Group × Angle interaction $p < 0.001$), resulting in significantly smaller AHD at 90° abduction ($p < 0.001$). Overall, lower sport classes were associated with lower measured shoulder performance and a different supraspinatus ultrasound profile. Well-characterized prospective cohorts are needed to determine the mechanisms and clinical relevance of these associations.

**Keywords:** para swimming; ultrasonography; supraspinatus tendon; acromiohumeral distance; rotator cuff strength

Check for updates

Academic Editors: Zhanneta Kozina and Valeria Tyshchenko

Received: 3 October 2026
Revised: 12 November 2026
Accepted: 13 November 2026
Published: 16 November 2026

**Copyright:** © 2026 by the authors. Licensee MDPI, Basel, Switzerland. This article is an open access article distributed under the terms and conditions of the Creative Commons Attribution (CC BY) license.

## 1. Introduction

Para swimming classification is intended to group athletes according to the extent to which an eligible impairment affects the execution of swimming-specific tasks. Athletes with physical impairments compete in sport classes S1–S10, with lower class numbers

generally representing greater activity limitation. However, sport class does not fully capture differences in impairment type, residual muscle function, joint mobility, coordination, trunk control and movement strategy [1]. This heterogeneity is particularly relevant in lower sport classes, in which substantial limitations of lower-limb and trunk function may restrict body alignment, rotation and force transmission between body segments. Consequently, upper-limb function may assume a greater role in propulsion and postural control, although the extent and nature of this dependence remain specific to the individual athlete [2–4].

For para swimmers who use a wheelchair for daily mobility, preserved shoulder function is critical for independent mobility and the performance of activities of daily living. Manual wheelchair use requires repeated upper-limb loading during propulsion, transfers, pressure-relief maneuvers, reaching, and other daily activities [4]. These tasks impose substantial and task-specific mechanical demands on the glenohumeral joint and the surrounding musculature and soft tissues [3–5]. Wheelchair propulsion requires the shoulder musculature to generate propulsive force while maintaining dynamic stability of the humeral head, whereas transfers and pressure-relief maneuvers involve weight-bearing through an anatomical complex primarily adapted for mobility rather than repetitive loading. Increased wheelchair propulsion velocity is also associated with greater shoulder joint forces and moments [3]. In wheelchair-using para swimmers, these daily demands are superimposed on the repetitive upper-limb cycles required in swimming, creating a distinct cumulative loading profile that cannot be inferred directly from studies of non-disabled swimmers or non-athletic wheelchair users [5].

Recent evidence indicates that upper-limb demands in wheelchair users are not uniform and may vary according to both propulsion strategy and sport-specific requirements [6]. Conventional pushing propulsion predominantly engages the anterior shoulder musculature, whereas pulling increases posterior upper-limb and trunk muscle activation and involves greater shoulder and elbow range of motion [5,7]. Moreover, wheelchair para-athletes may demonstrate discipline-dependent interlimb asymmetries in shoulder strength and range of motion, reflecting the interaction between habitual wheelchair use, impairment-related motor constraints and sport-specific technical demands [7]. These findings support bilateral shoulder assessment and context-specific interpretation of musculoskeletal screening outcomes in wheelchair-using para swimmers.

The rotator cuff, particularly the supraspinatus tendon, and the long head of the biceps tendon are frequently affected in manual wheelchair users. Ultrasound studies have demonstrated structural and echogenic abnormalities of the tendons, tendinopathy, and partial-thickness tears involving the rotator cuff tendons and the long head of the biceps. Magnetic resonance imaging studies have likewise indicated a high prevalence of rotator cuff tendinopathy and tendon tears, as well as tendinopathy of the long head of the biceps tendon, although tears of the latter were less common [8,9]. Importantly, imaging abnormalities are not consistently associated with current pain or perceived disability. Structural changes may be present in minimally symptomatic or asymptomatic wheelchair users, and reliance on self-reported pain alone may therefore underestimate shoulder tissue involvement [8–10]. This discrepancy is clinically relevant in athletes, who may continue to train despite symptoms, modify their movement strategies, or regard shoulder discomfort as an unavoidable consequence of wheelchair use and sport.

Subacromial morphology may provide additional information about the mechanical environment of the rotator cuff. Acromiohumeral distance describes the space between the acromion and humeral head, whereas the occupation ratio expresses supraspinatus tendon thickness relative to available subacromial space. In manual wheelchair users, ultrasound measurements of supraspinatus tendon thickness and occupation ratio differ from those obtained in non-wheelchair controls, suggesting tissue adaptation associated

with prolonged upper-limb use [11]. Nevertheless, neither acromiohumeral distance nor occupation ratio should be considered a stand-alone diagnostic marker of impingement or a direct explanation of pain. These measures should instead be interpreted as morphological characteristics within a broader assessment that considers tendon structure, symptoms, functional demands, impairment profiles and exposure to wheelchair and sport-related loading [12].

Evidence on shoulder morphology in para swimmers remains scarce. In a preliminary study of athletes competing in higher functional classes (S7–S10), Klich et al. observed greater supraspinatus tendon thickness in athletes with upper-limb impairments than in those with lower-limb impairments or non-disabled controls; the occupation ratio was also higher in the upper-limb impairment group than in the lower-limb impairment group [12]. More recently, para swimmers with chronic rotator cuff tendinopathy were shown to differ from asymptomatic controls in supraspinatus tendon thickness, PSFR-derived micromorphological characteristics, acromiohumeral distance and occupation ratio [13]. However, both studies involved athletes from relatively high functional classes and focused either on specific impairment profiles or established tendinopathy. Therefore, the extent to which these findings apply to wheelchair-using swimmers from lower sport classes and with more pronounced activity limitations remains uncertain [14].

Musculoskeletal ultrasound offers several practical advantages for shoulder screening in para sport. It is non-invasive, portable, relatively accessible, and suitable for bilateral examination in a sports environment. Standardized protocols can provide reliable measurements of supraspinatus and long-head biceps tendon morphology, acromiohumeral distance and subacromial occupation ratio [11,13–15]. Ultrasound can also identify findings that may warrant further clinical assessment, including tendon disorganization, focal defects, calcification, bursal fluid, or fluid surrounding the long head biceps tendon. However, screening findings should not be interpreted as definitive diagnoses or direct indicators of tissue damage. Their relevance depends on the measurement protocol, examiner reliability, athlete characteristics, symptoms, and clinical examination [14,16–19].

To date, shoulder imaging research has primarily examined non-athletic manual wheelchair users, wheelchair court-sport athletes, non-disabled swimmers, or para swimmers from comparatively high functional classes. To confirm the extent of the available literature, we conducted searches in main databases, e.g., PubMed, SPORTDiscus, and Web of Science using combinations of terms including: “para swimming”, “wheelchair”, “shoulder”, “ultrasound”, and “lower sport class”. To our knowledge, the shoulder status of wheelchair-using para swimmers from lower sport classes has not been systematically characterized in a screening context. Consequently, our current understanding of shoulder health in this population relies entirely on extrapolating evidence from adjacent athletic and non-athletic cohorts. The present study addresses this evidence gap by comparing shoulder functional performance and ultrasonographic characteristics between para swimmers classified as S1–S6 and S7–S10. These comparisons may provide further insight into the variation in shoulder characteristics across distinct functional and mobility profiles. This represents a critical evidence gap, because wheelchair-dependent athletes experience unique cumulative dual-loading from daily mobility and sport-specific upper-limb demands. Comparing this group to higher-functioning, predominantly ambulatory para swimmers provides a unique opportunity to evaluate how these varying functional demands influence shoulder morphology. Therefore, the primary objective of this cross-sectional ultrasonographic screening study was to compare the structural characteristics of the shoulder complex with particular attention to the supraspinatus tendon and the subacromial space between wheelchair-dependent para swimmers from lower sport classes (S1–S6) and ambulatory para swimmers from higher sport classes (S7–S10). It was hypothesized that athletes in the

lower-level functional class would exhibit reduced peak force, lower rate of force development (RFD), and decreased active range of motion (ROM) compared to the higher-level class. Furthermore, we hypothesized that the lower-level group would demonstrate altered structural characteristics, specifically greater supraspinatus tendon thickness and occupation ratio, alongside a reduced acromiohumeral distance (AHD). Establishing the prevalence and distribution of ultrasound findings in this under-researched population may support more targeted clinical follow-up, shoulder health surveillance, preventive rehabilitation, and long-term training management.

## 2. Materials and Methods

### *2.1. Study Design*

The present study employed a cross-sectional comparative design to systematically evaluate the biomechanical and morphological characteristics of the shoulder girdle, with a specific focus on the rotator cuff in wheelchair users. This methodological design includes an inter-group comparison across one independent factor, i.e., functional class status (lower-level vs. higher-level functional classes) in elite para swimmers.

Participants underwent laboratory testing, including shoulder strength measurements (peak force [N] and rate of force development [N/s], range of motion (ROM) [°], and macro-morphological properties, i.e., supraspinatus tendon (SST) thickness [mm], acromiohumeral distance at 0°, 60°, and 90°, as well as occupation ratio [%]. To prevent acute, load-induced alterations in tendon dimensions, all baseline and dynamic ultrasound imaging was completed prior to any maximal strength or active range of motion testing within the session. Additionally, peak spatial frequency radius (PSFR, $mm^{-1}$) was quantified as an ultrasound image-texture parameter.

Before the data collection, each participant was instructed to abstain from upper-extremity resistance training, as well as high-intensity or high-volume swimming protocols, for a minimum of 48 h prior to data acquisition. All ultrasonographic assessments were performed on the dominant upper extremity by a single clinician with 10 years of specialized expertise in musculoskeletal ultrasound, thereby maximizing procedural consistency and eliminating inter-rater variability. The study was conducted following STROBE guidelines [20] and in strict accordance with the ethical principles outlined in the Declaration of Helsinki. Written informed consent was obtained from all participants before enrollment, following formal protocol approval by the Senate Research Ethics Committee (Project Identification Code: 07/2026).

### *2.2. Participants*

Forty elite senior swimmers (aged 18–35 years) were recruited from the Polish National Para Swimming Team. All participants were right-handed and had previously competed at the junior and senior European and World Championships. Participants were classified into two groups, i.e., lower-level functional-class para swimmers (n = 20) and higher-level functional-class para swimmers (n = 20). Detailed demographic and training profiles are provided in Table 1. Swimmers classified in the S1–S6 group used manual wheelchairs as their primary means of daily mobility (mean duration of use: 20 ± 5 years). Conversely, participants in the S7–S10 group were ambulatory and did not rely on a manual wheelchair for daily mobility.

**Table 1.** Participant characteristics by functional-class group.

| Variable | Lower Group | Upper Group | Mean Difference (95% CI) | *p*-Value |
|---|---|---|---|---|
| Age (year) | 26 ± 5.3 | 23 ± 3.0 | 3.00 (0.25 to 5.75) | 0.034 |
| Sex | ♂: 10; ♀: 10 | ♂: 10; ♀: 10 | | |
| Body height (cm) | 160.5 ± 5.1 | 173 ± 4.2 | −12.50 (−15.47 to −9.53) | <0.001 |
| Body mass (kg) | 65.6 ± 5.0 | 73.3 ± 6.4 | −7.70 (−11.39 to −4.01) | <0.001 |
| Body mass index (kg/m$^2$) | 23 ± 1.5 | 23 ± 1.3 | 0.00 (−0.88 to 0.88) | 1.000 |
| Training experience (years) | 10 ± 5 | 12 ± 3 | −2.00 (−4.65 to 0.65) | 0.135 |
| **Exposure and Classification** | | | | |
| Sport Class Distribution (n) | S1: [0], S2: [4], S3: [4]; S4: [4], S5: [4], S6: [4] | S7: [4], S8: [4]; S9: [6], S10: [6] | | |
| Manual wheelchair use (years) | 20 ± 5 | N/A | | |
| Weekly swimming volume (number of training sessions per week) | 9 ± 0 | 9 ± 0 | 0.00 (0.00 to 0.00) | 1.000 |

Overall, inclusion criteria for both groups were: (1) medical classification in either the low functional class (S1 to S6) or high functional class (S7 to S10), including specific physical impairments, e.g., the S1 to S6 classes include swimmers with severe motor limitations, such as severe tetraplegia or four-limb motor loss (S1); severe coordination impairment with minimal trunk control (S2); amputation of three or four limbs or severe diplegia (S3); severe trunk impairment with limited hand/arm function (S4); complete loss of trunk control or severe paraplegia (S5); and short stature (such as achondroplasia), bilateral above-knee amputations, or moderate trunk impairment (S6); whereas the S7 to S10 classes include swimmers with moderate to minimal impairments, such as paralysis or loss of one arm or severe hip/knee joint restrictions (S7); single-upper-extremity amputation above/below the elbow or double-lower-extremity loss below the knee (S8); unilateral lower limb amputation or moderate joint restrictions (S9); and minimal physical impairments, such as mild leg length discrepancies or loss of a foot (S10); (2) active competitive swimming training experience (e.g., >2 years). The exclusion criteria included: (1) current or previous dominant shoulder injury, impingement symptoms, or rotator cuff pathology; (2) prior history of surgery or major dislocation in the shoulder girdle; (3) acute cardiovascular or systemic contraindications to maximal exercise. According to the medical classification point system, the S1 to S6 low functional classes include swimmers scoring between 0 and 190 points, characterized by severe trunk and multi-limb restrictions, absent or limited dynamic sitting balance, and minimal lower-extremity propulsion. Specifically, classes S1 to S3 encompass swimmers with extreme functional limitations relying almost exclusively on modified head and partial arm movements (scoring 0 to 150 points), while classes S4 to S6 include swimmers with moderate-to-severe trunk impairment or short stature (scoring 151 to 190 points). Conversely, the S7 to S10 high functional classes encompass swimmers scoring between 191 and 300 points, characterized by partial to full dynamic trunk control and active lower-limb propulsion. Class S7 includes swimmers scoring between 191 and 215 points, typically presenting with single-arm paralysis or severe lower-limb joint contractures. Class S8 encompasses swimmers scoring from 216 to 240 points, characterized by single upper-extremity amputation above the elbow or dysmelia. Swimmers classified as S9 (scoring 241 to 265 points) and S10 (scoring 266 to 300 points) exhibit single-limb distal loss or mild joint restrictions, with S10 representing those with minimal physical impairments [1]. Eligibility required a physical-impairment sport class within S1–S10 and more than two years of competitive swimming training. Participants were grouped as S1–S6 or S7–S10 for the present between-group comparison. These categories describe broad sport-class ranges; they do not define homogeneous clinical phenotypes or a common level of trunk control, lower-limb function, or shoulder loading. Sport classification reflects

the impact of an eligible impairment on swimming-specific activities rather than a single diagnosis or a uniform biomechanical profile [1]. In the present cohort, the S1–S6 group used manual wheelchairs for daily mobility, whereas the S7–S10 group was ambulatory. These are characteristics of the recruited participants and should not be generalized to all athletes in these sport classes. Accordingly, the between-group comparison cannot isolate associations with sport class from differences in mobility status or impairment characteristics. Exclusion criteria were current or previous dominant-shoulder injury, impingement symptoms, or rotator cuff pathology; previous shoulder-girdle surgery or major dislocation; and acute cardiovascular or systemic contraindications to maximal exercise.

A sensitivity analysis was conducted utilizing G*Power software (version 3.1.9.2; Heinrich-Heine-Universität Düsseldorf, Düsseldorf, Germany). The estimation was based on detecting between-group differences (lower-level vs. higher-level functional classes) using an Analysis of Variance (ANOVA). To stringently control for statistical errors, the parameters were predefined with an alpha level ($\boldsymbol{\alpha}$) of 0.05, a target statistical power ($\mathbf{1} - \boldsymbol{\beta}$) of 0.90, and a minimum expected effect size (Cohen's $\boldsymbol{f}$) of 0.30. Based on these parameters, the algorithm determined that a minimum total sample size of n = 40 (n = 20 per functional group) was necessary. Consequently, exactly 40 para-swimmers were recruited and took part in the study proceedings, fulfilling the a priori sample size requirement.

### *2.3. Experimental Procedure*

#### 2.3.1. Rotator Cuff Muscle Strength

Isometric force generation during upper-extremity tests was measured using the DynaMo digital dynamometer system (VALD Performance, Brisbane, QLD, Australia). The device incorporates a combined tension and compression load cell sensor alongside a 3D inertial measurement unit (IMU). Force data were sampled continuously at a frequency of 1200 Hz and transmitted wirelessly via Bluetooth to the DynaMo mobile application (VALD Hub, version 2.x, VALD, Brisbane, Australia) for real-time capture and cloud storage. To eliminate examiner strength bias and minimize artifact from tester movement, the DynaMo unit was anchored to an immovably fixed structural rig using high-tensile, non-compliant stabilization straps rather than being held manually by the investigator. Before each testing session, the device load cell was auto-zeroed in the test position to account for strap mass and baseline tension [17,18,21].

All assessments were conducted on the dominant upper extremity under standardized environmental conditions. Participants performed two isometric assessments. For shoulder abduction, participants sat supported by a wheelchair backrest (lower group) or chair backrest (upper group) with feet shoulder-width apart, knees slightly flexed, and the spine in a neutral posture. The target shoulder was positioned at 90 degrees of abduction in the frontal plane, with the elbow fully extended (0 degrees) and the forearm in a neutral pronation-supination position. The DynaMo device force pad was placed lateral to the upper arm, precisely 2 cm proximal to the lateral epicondyle of the humerus. A stabilization strap anchored to a rigid vertical frame held the unit in position to resist upward movement during abduction. A secondary stabilization belt was placed across the contralateral shoulder and pelvis to prevent lateral trunk flexion or compensatory body lean during exertion. For shoulder pull, participants were positioned in a seated or standing posture facing the fixed frame. The testing shoulder was placed in 90 degrees of shoulder flexion and 0 degrees of horizontal adduction, with the elbow flexed at 90 degrees. The DynaMo unit was configured in tension mode using the attachment loop. A non-compliant strap extended from the device to a padded cuff placed around the distal forearm (2 cm proximal to the radial styloid process). Belt stabilization was applied across the thorax to isolate scapulothoracic and glenohumeral pull mechanics and prevent posterior trunk extension [17,18].

Participants completed a 5-min dynamic upper-body warm-up consisting of arm circles, shoulder band dislocations, and low-intensity submaximal isometric contractions (50% and 75% perceived effort). Prior to formal data collection, participants completed two submaximal practice trials per test movement to ensure familiarization with the rigid isometric resistance. Participants then performed three maximal voluntary isometric contractions (MVIC) for each test movement (shoulder abduction and pull). Standardized verbal encouragement was delivered. Each trial lasted 5 s, comprising an explosive onset followed by sustained maximal effort. A 120-s passive recovery period was enforced between individual trials to prevent neuromuscular fatigue. Test order between abduction and pull was randomized using a computer-generated block randomization sequence.

Force-time curves generated during each MVIC trial were exported at 1200 Hz and smoothed using a zero-lag, low-pass fourth-order Butterworth filter with a 15 Hz cutoff frequency. The primary outcome variables were: Peak Force (PF, in Newtons): The single maximum instantaneous force value recorded during the 5-s MVIC period. Peak Rate of Force Development (Peak RFD, in N/s): The maximum slope of the force-time curve calculated using a moving 20 ms window ($\Delta F/\Delta t$). To eliminate proportional bias between groups with differing absolute strength, force onset (t0) was strictly defined using a single absolute threshold, identified as the point where force exceeded baseline by 5 N. Note: Time-specific RFD intervals such as 0–50 ms and 0–100 ms were computed but are excluded from this report to focus specifically on maximal explosive capacity.

#### 2.3.2. Shoulder Range of Motion

Active shoulder flexion and abduction range of motion (ROM) were measured using a wired twin-axial electrogoniometer (Noraxon USA Inc., Scottsdale, AZ, USA). Participants were assessed in a seated position adapted to their functional abilities. The starting position was with the testing arm alongside the body and the thumb pointing forward. To measure the full arc of active elevation, the electrogoniometer's stationary plate was attached to the lateral midline of the thorax and the movable plate to the lateral midline of the humerus via a flexible shim. Following familiarization, participants performed active shoulder flexion and abduction. Positioning was standardized to minimize compensatory trunk movement. For muscle strength assessment, participants performed maximal voluntary isometric contractions against a fixed dynamometer in the respective planes of movement. Device settings, sensor placements, and measurement procedures followed previously described protocols [17,18]. Three trials were recorded for each movement, and their mean was used in the analysis.

#### 2.3.3. Rotator Cuff Ultrasound Imaging

Ultrasound imaging of the rotator cuff structures was performed using a high-resolution diagnostic ultrasound system (Alpinion X-CUBE 90, Alpinion, Seoul, Republic of Korea) equipped with a 60 mm linear array transducer (3.0 to 19.0 MHz; SL3-19X; X+ Crystal Signature; Alpinion) in grey-scale B-mode. For optimal imaging of macro-morphological properties, a high-frequency setting of 18 MHz was selected. For speckle tracking of the micro-morphology (i.e., PSFR), a lower transducer frequency of 8 MHz was utilized. The ultrasound machine was preset for musculoskeletal imaging with opacity set at 100%, depth at 2 to 4 cm to frame the tendon insertion with an extra 1 cm of the humeral head, focus placed at 1 to 2 cm depth for sharp resolution, and overall gain adjusted to 50 to 70% with time gain compensation (TGC) curved upward near the superficial tendon to ensure uniform brightness without saturation. Images were captured by a single certified physical therapist with a practice in musculoskeletal ultrasonography (10 years of experience). The

ultrasound procedures and measurements, both for macro- and micro-morphology of the rotator cuff, were made according to Pożarowszczyk-Kuczko et al. [13].

Participants were assessed in a seated position with their lower back supported. For SST thickness and PSFR imaging, the arm was positioned alongside the body with the thumb pointing forward. For AHD measurements, the arm initially rested on the thigh at 0° of shoulder abduction. AHD was then measured at 60° and 90° of abduction. At these elevated positions, the investigator passively positioned the arm, verified the angle using a clinical goniometer, and supported the arm on an adjustable stand during image acquisition. Participants were informed about the measurement procedures before data collection [12,14].

During the SST examination, the transducer was moved anteriorly and laterally until the most distal end of the SST and the hyperechoic greater tuberosity were identified. In the longitudinal view, the SST appeared as a beak-shaped structure with a fibrillar pattern and regular margins. The transducer was gently moved side to side with slight pressure toward the participant's body, orienting it approximately 45 degrees between the sagittal and frontal planes. The SST boundaries were defined as the most hyperechoic area above the anechoic articular cartilage of the humeral head and the hyperechoic upper edge of the tendon anterior to the anechoic subacromial–subdeltoid bursa. For the AHD images, the transducer was placed on the anterior acromial margin to identify the anterolateral aspect, allowing for the visualization of the inferior aspect of the acromion and the superior aspect of the humeral head [14].

The SST thickness was analyzed segmentally at standardized locations measured proximal to the tendon's insertion on the greater tuberosity. The primary anatomical landmark is established at the distal insertion site, defined as the point where the hyperechoic bony cortex of the greater tuberosity meets the anechoic articular cartilage of the humeral head. From this baseline insertion point, segmental thickness measurements were taken along the longitudinal axis of the tendon at 5 mm, 10 mm, and 15 mm proximal to the attachment site. At each specific reference point, a digital linear caliper was placed perpendicularly from the superior hyperechoic margin of the tendon beneath the subacromial–subdeltoid bursa down to the deep hyperechoic boundary above the humeral cartilage or bony surface. Three distinct longitudinal B-mode images are captured per participant, and the segmental thickness values at 5 mm, 10 mm, and 15 mm are averaged across trials to establish both point-specific and overall supraspinatus tendon thickness metrics [12,17].

For the assessment of the AHD, it was defined as the shortest linear perpendicular distance in millimeters measured from the most inferior hyperechoic point of the acromion down to the most superior hyperechoic apex of the humeral head. Three trials were captured, and the resulting measurements were averaged to determine the representative distance. To calculate the occupation ratio, divide the supraspinatus tendon thickness in millimeters by the acromiohumeral distance measured at 0 degrees of shoulder abduction in millimeters, and multiply the result by 100. It represents the percentage proportion of the subacromial space occupied by the tendon tissue [17].

Finally, for the PSFR measurements, each ultrasound image was stored as a DICOM file and further processed using MicroDicom Viewer (MicroDicom Ltd., Sofia, Bulgaria) to extract the best view from a 6-s loop as a JPG file. Analysis was conducted using a custom MATLAB 2026b algorithm (MathWorks, Natick, MA, USA) employing Spatial Frequency Analysis (SpaFTA 2.6). A region of interest (ROI) defined the entire tendon from the humeral head to the bursal layer of the subdeltoid bursa. Three kernels were placed at the most echogenic areas of the tendon at 5, 10, and 15 mm from the greater tuberosity. The kernels measured 24 × 24 pixels (1.05 × 1.05 mm) at 5 mm, 32 × 32 pixels (1.4 × 1.4 mm) at 10 mm, and 38 × 38 pixels (1.66 × 1.66 mm) at 15 mm. Kernels were

zero-padded to 128 × 128 samples, and a 2D Fast Fourier Transform was applied with a 2D high-pass filter (3 dB cutoff frequency of approximately 1.0 $mm^{-1}$) to reduce low spatial frequency artifacts. The PSFR values obtained from the three kernels were averaged to provide a quantitative measure of the spatial frequency characteristics of the ultrasound image. Higher PSFR values indicate greater high-spatial-frequency content within the analyzed regions. However, this image-derived parameter does not independently establish collagen disorganization, tendon degeneration, or histopathological alterations [14,22–26].

### *2.4. Statistical Analysis*

Statistical analyses were performed using SPSS software (version 28.0; IBM Corp., Armonk, NY, USA). Continuous variables for all demographic, functional, and morphological parameters were expressed as mean values, standard deviations, and ninety-five percent confidence intervals (95% CI). Between-group baseline differences in age, body height, body mass, and training experience were assessed using independent-samples *t*-tests. Normality of data distribution was assessed using the Shapiro–Wilk test, and homogeneity of variances was evaluated using Levene's test. For group comparisons, conventional independent-samples *t*-tests were utilized for variables that met all parametric assumptions (SST, OR). For parameters exhibiting significant heterogeneity of variances despite a normal distribution (Peak force pull, Peak force abduction), Welch's *t*-test was conducted. Finally, for variables that presented significant deviations from normality (active ROM flexion, active ROM abduction, RFD pull, RFD abduction, and PSFR), the non-parametric Mann–Whitney U test was applied, and results were expressed as medians and interquartile ranges (IQR).

Intra-rater reliability across three consecutive trials conducted by a single investigator was evaluated using the Intraclass Correlation Coefficient, model ICC (A,1), based on a two-way mixed-effects model with single-measurement and absolute agreement. Reliability was independently assessed across all outcome measures, including muscle strength metrics of peak force and RFD during shoulder pull and abduction, active ROM during shoulder flexion and abduction, macro-morphological ultrasound parameters encompassing SST thickness, AHD, and occupation ratio, as well as micro-morphological properties represented by the PSFR. Point estimates for ICC were categorized as excellent for values equal to or greater than 0.90, good for values between 0.75 and 0.89, moderate for values between 0.50 and 0.74, and poor for values below 0.50. Measurement error and precision were quantified by calculating the Standard Error of Measurement (SEM), the Minimal Detectable Change at the 95% ($MDC_{95}$) confidence level, and the relative coefficient of variation.

The intra-rater reliability estimates were derived directly from the three consecutive trials completed by each participant. For the primary between-group analyses, a single representative metric was subsequently extracted from these same three trials. Specifically, for all ultrasound morphological parameters (SST thickness, AHD, occupation ratio, PSFR) and range of motion measurements, the mean of the three trials was calculated and utilized. For isometric muscle strength (peak force and RFD), the highest value achieved across the three trials was selected. For the evaluation of inter-group differences via independent-samples *t*-tests, outcomes were explicitly categorized based on the study's primary objective. Macro- and micro-morphological ultrasound parameters (SST thickness, occupation ratio, and PSFR) were designated as the primary outcomes, whereas functional measures (shoulder strength and active ROM) were treated as secondary, exploratory outcomes intended to contextualize the structural findings. While a formal family-wise error rate correction was not applied across all secondary *t*-tests due to their exploratory nature, it should be noted that all observed inter-group differences yielded highly significant *p*-values ($p \leq 0.004$) that would inherently survive standard false-discovery rate adjustments. Specifically, this

analysis was performed for shoulder strength, active ROM, SST thickness, occupation ratio, and PSFR. However, to investigate the relationship between AHD across different shoulder abduction angles and functional class status groups, a two-way mixed-design analysis of variance (2 *Groups* [lower-level vs. higher-level] × 3 *abduction angles* [0°, 60°, and 90°]) was conducted. This model evaluated the main effect of functional class group, the main effect of shoulder abduction angle, and the *Group* by *Angle* interaction effect on AHD. Assumptions of sphericity for the within-subject factor of abduction angle in the mixed ANOVA models were assessed using Mauchly's test, and a Greenhouse-Geisser correction was applied whenever the assumption of sphericity was violated. When statistically significant main effects or *Group* by *Angle* interaction effects were detected, pairwise post hoc comparisons were executed using Bonferroni adjustments to control for Type I error. Effect sizes (Cohen's d) were calculated using the higher-level functional class (S7–S10) as the reference baseline (i.e., lower-level group mean minus higher-level group mean). Consequently, negative d values indicate lower measured values in the lower-level group, whereas positive d values indicate higher measured values in the lower-level group. Effect sizes for the mixed-design ANOVA main and interaction effects were calculated and reported using partial eta squared ($\eta_p^2$). For all statistical tests, the significance level was established at a two-tailed alpha of 0.05.

## 3. Results

### *3.1. Rotator Cuff Muscle Strength*

Intra-rater reliability for shoulder pull peak force was excellent, with an ICC (A,1) of 0.94 (95% CI: 0.89 to 0.97), an SEM of 5.21 N, and a $MDC_{95}$ of 14.44 N. Abduction peak force demonstrated excellent intra-rater reliability (ICC (A,1) = 0.92, 95% CI: 0.86 to 0.96; SEM = 7.18 N; $MDC_{95}$ = 19.90 N). Shoulder pull RFD was good (ICC (A,1) = 0.88, 95% CI: 0.79 to 0.93), exhibiting an SEM of 32.65 N/s and an $MDC_{95}$ of 90.50 N/s. Finally, abduction RFD exhibited good intra-rater reliability (ICC (A,1) = 0.85, 95% CI: 0.74 to 0.92; SEM = 39.81 N/s; $MDC_{95}$ = 110.35 N/s).

The higher-level functional class group demonstrated significantly higher peak force during the shoulder pull (219.40 ± 30.78 N) compared to the lower-level functional class group (100.30 ± 7.06 N). Due to significant heterogeneity of variances, Welch's *t*-test was utilized, confirming a statistically significant difference ($t(20.99) = -16.87$, $p < 0.001$), with an extremely large effect size ($d = -5.33$) and a 95% confidence interval for the mean difference of −133.78 N to −104.42 N. Analysis of shoulder abduction peak force revealed significantly greater strength in the higher-level group (163.00 ± 32.96 N) relative to the lower-level group (93.70 ± 7.53 N). Welch's *t*-test confirmed this substantial inter-group difference ($t(20.98) = -9.17$, $p < 0.001$), highlighting a large effect size ($d = -2.90$) and a 95% confidence interval of −85.02 N to −53.58 N (Table 2).

**Table 2.** Descriptive statistics and independent-samples *t*-test results comparing functional class groups.

| Variable | Lower-Level (Mean ± SD) | Higher-Level (Mean ± SD) | Test Statistic | *p*-Value | Effect Size |
|---|---|---|---|---|---|
| **Muscle Strength** | | | | | |
| Peak Force Pull (N) | 100.30 ± 7.06 | 219.40 ± 30.78 | t(20.99) = −16.87 | <0.001 | d = −5.33 |
| Peak Force Abduction (N) | 93.70 ± 7.53 | 163.00 ± 32.96 | t(20.98) = −9.17 | <0.001 | d = −2.90 |
| Peak RFD Pull (N/s) | 222.10 ± 44.0 * | 595.05 ± 118.37 * | U = 0.00 | <0.001 | r = 1.00 |
| Peak RFD Abduction (N/s) | 131.60 ± 25.48 * | 345.00 ± 140.75 * | U = 1.00 | <0.001 | r = 0.99 |
| **Range of Motion** | | | | | |
| ROM Flexion (°) | 142.45 ± 28.48 * | 173.60 ± 4.65 * | U = 57.50 | <0.001 | r = 0.71 |
| ROM Abduction (°) | 150.95 ± 22.86 * | 166.85 ± 4.06 * | U = 115.00 | 0.022 | r = 0.43 |

**Table 2.** *Cont.*

| Variable | Lower-Level (Mean ± SD) | Higher-Level (Mean ± SD) | Test Statistic | *p*-Value | Effect Size |
|---|---|---|---|---|---|
| **Ultrasound imaging** | | | | | |
| SST Thickness (mm) | 5.93 ± 0.54 | 4.89 ± 0.49 | t(38) = 6.29 | <0.001 | d = 2.02 |
| Occupation ratio (%) | 62.70 ± 6.17 | 51.10 ± 5.46 | t(38) = 6.30 | <0.001 | d = 1.99 |
| PSFR ($mm^{-1}$) | 2.21 ± 0.25 * | 1.42 ± 0.28 * | U = 398.00 | <0.001 | r = 0.99 |

* Note: Normally distributed variables with equal variances (SST, occupation ratio) are presented as Mean ± Standard Deviation, analyzed via Student's *t*-test with Cohen's d effect size. Normally distributed variables with unequal variances (peak force) are presented as Mean ± Standard Deviation, analyzed via Welch's *t*-test with Cohen's d effect size. Non-normally distributed variables (denoted with *) are presented as Median (Interquartile Range) and analyzed using the Mann–Whitney U test with rank-biserial correlation (r) for effect size. Legend—SD = standard deviation; CI = confidence interval; RFD = rate of force development; ROM = range of motion; SST = supraspinatus tendon; OR = subacromial space occupation ratio; PSFR = peak spatial frequency radius; d = Cohen's d standardized effect size.

For RFD, the higher-level functional class showed a significantly higher Peak RFD during the shoulder pull (Median = 581.00 N/s, IQR = 176.25 N/s) than the lower-level class (Median = 220.50 N/s, IQR = 75.25 N/s). This outcome was highly significant ($U = 0.00$, $p < 0.001$), producing a near-perfect rank-biserial effect size ($r = 1.00$). Abduction RFD was also significantly elevated in the higher-level group (Median = 331.00 N/s, IQR = 206.75 N/s) compared to the lower-level group (Median = 131.00 N/s, IQR = 30.50 N/s). Statistical testing confirmed this outcome ($U = 1.00$, $p < 0.001$), alongside a very large rank-biserial effect size ($r = 0.99$) (Table 2).

### 3.2. Shoulder Range of Motion

Intra-rater reliability for flexion showed excellent intra-rater reliability (ICC (A,1) = 0.96, 95% CI: 0.92 to 0.98), with an SEM of 4.12° and an $MDC_{95}$ of 11.42°, while abduction presented excellent intra-rater reliability (ICC (A,1) = 0.93, 95% CI: 0.87 to 0.96; SEM = 4.50°; $MDC_{95}$ = 12.47°).

Active shoulder flexion ROM was significantly greater for participants in the higher-level group (Median = 174.0°, IQR = 4.75°) compared to those in the lower-level group (Median = 149.0°, IQR = 49.50°). A Mann–Whitney U test yielded a significant result ($U = 57.50$, $p < 0.001$), with a large rank-biserial effect size ($r = 0.71$). The higher-level functional class group displayed significantly greater active shoulder abduction ROM (Median = 168.0°, IQR = 5.00°) relative to the lower-level group (Median = 155.0°, IQR = 26.75°). This difference was statistically significant ($U = 115.00$, $p = 0.022$), reflecting a moderate-to-large effect size ($r = 0.43$) (Table 2).

### 3.3. Rotator Cuff Ultrasound Imaging

Ultrasound measurement of SST thickness displayed excellent intra-rater reliability (ICC (A,1) = 0.91, 95% CI: 0.84 to 0.95), with an SEM of 0.16 mm and an $MDC_{95}$ of 0.44 mm. The occupation ratio showed good intra-rater reliability (ICC (A,1) = 0.89, 95% CI: 0.81 to 0.94; SEM = 1.95%; $MDC_{95}$ = 5.41%). The AHD demonstrated excellent intra-rater reliability (ICC (A,1) = 0.93, 95% CI: 0.83 to 0.97), with an SEM of 0.19 mm and an $MDC_{95}$ = 0.53 mm. Finally, the PSFR showed good intra-rater reliability (ICC (A,1) = 0.86, 95% CI: 0.76 to 0.92; SEM = 0.10 $mm^{-1}$; $MDC_{95}$ = 0.28 $mm^{-1}$).

Ultrasound macro-morphological assessment indicated that the lower-level functional class group possessed a significantly thicker SST (5.93 ± 0.54 mm) than the higher-level group (4.89 ± 0.49 mm). This morphological difference was highly significant, $t(38) = 6.29$, $p < 0.001$, with a large effect size ($d = 2.02$) and a 95% confidence interval for the difference between 0.70 mm and 1.37 mm (Table 2).

The occupation ratio was significantly higher in the lower-level group (62.70 ± 6.17%) compared to the higher-level group (51.10 ± 5.46%). The independent-samples analysis confirmed a statistically significant between-group difference in occupation ratio, $t(38) = 6.30$, $p < 0.001$, demonstrating a large effect size ($d = 1.99$) and a 95% confidence interval of 7.87% to 15.33% (Table 2).

Micro-morphological analysis revealed significantly higher PSFR values in the lower-level functional class group (Median = 2.19 $mm^{-1}$, IQR = 0.22 $mm^{-1}$) than in the higher-level group (Median = 1.47 $mm^{-1}$, IQR = 0.21 $mm^{-1}$). This ultrasonographic distinction in spatial structural properties was statistically significant ($U = 398.00$, $p < 0.001$), yielding a very large rank-biserial effect size ($r = 0.99$) (Table 2).

A two-way mixed-design ANOVA was conducted to evaluate the effects of functional class status *Groups* and shoulder abduction *Angles* on the AHD. The analysis revealed a statistically significant main effect of the shoulder abduction *Angle* on the AHD ($F(2,76) = 64.58$, $p < 0.001$, $\eta_p^2 = 0.630$), indicating that the distance significantly decreases as the shoulder joint elevated. Furthermore, a significant main effect of the functional class *Group* was observed ($F(1,38) = 46.27$, $p < 0.001$, $\eta_p^2 = 0.549$), demonstrating overall differences in the AHD between the lower-level and higher-level cohorts. Furthermore, the interaction effect between the functional class *Group* and the shoulder abduction *Angle* was also statistically significant ($F(2,76) = 15.14$, $p < 0.001$, $\eta_p^2 = 0.285$), confirming that the trajectory of AHD reduction during shoulder abduction differs significantly depending on the swimmer's functional class status. Within the lower-level group, the AHD decreased significantly from 0° to 60° (mean difference = 0.85 mm, adjusted $p < 0.001$), further decreased significantly from 60° to 90° (mean difference = 0.94 mm, adjusted $p < 0.001$), and showed a highly significant overall reduction from 0° to 90° (mean difference = 1.79 mm, adjusted $p < 0.001$). Within the higher-level group, the acromiohumeral distance remained stable between 0° and 60° (adjusted $p = 1.000$); however, a significant reduction occurred when elevating from 60° to 90° (mean difference = 0.57 mm, adjusted $p = 0.001$). Between groups at specific angles, there were no statistically significant differences in the acromiohumeral distance at 0° of abduction (adjusted $p = 1.000$); however, as abduction increased, the higher-level group exhibited a significantly greater AHD compared to the lower-level group at both 60° (mean difference = 0.88 mm, adjusted $p < 0.001$) and 90°(mean difference = 1.26 mm, adjusted $p < 0.001$) (Figure 1).

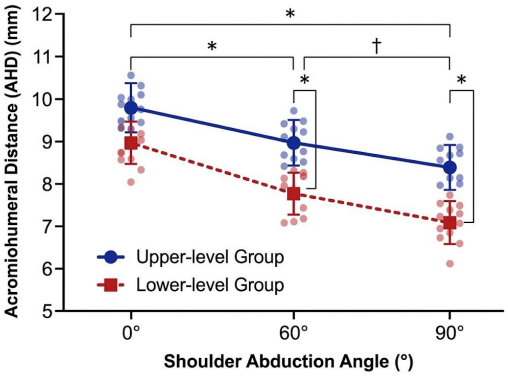



**Figure 1.** Mean (±SD) acromiohumeral distance for higher-level and lower-level swimmers across shoulder abduction angles. **Between-group comparisons:** * $p < 0.001$ indicates a statistically significant difference between the higher-level and lower-level groups at 90° of abduction. No significant between-group differences were observed at 0° ($p = 1.000$) or 60° ($p = 0.228$). **Within-group angle progressions:** † $p < 0.05$ indicates a statistically significant decrease in acromiohumeral distance across abduction angles within a single group. In the lower-level group, significant space reduction occurred from 0° to 60° ($p < 0.001$), 60° to 90° ($p < 0.001$), and 0° to 90° ($p < 0.001$). In the higher-level group, a significant reduction occurred between 60° and 90° ($p = 0.011$).

## 4. Discussion

This cross-sectional study identified differences in task-specific dominant-shoulder performance and ultrasound measurements between para swimmers grouped as S1–S6 and S7–S10. The S1–S6 group had lower peak force and rate of force development during the pull and abduction tests, lower active flexion and abduction ROM, and greater SST thickness, occupation ratio, and PSFR. AHD was smaller in the S1–S6 group at 90° of abduction, whereas no statistically significant between-group difference was detected at 0° or 60°. These findings describe associations between the athletes' combined functional and mobility profiles and specific shoulder characteristics within the recruited cohort, and do not identify their causes or establish shoulder pathology.

The functional differences were substantial: mean pull peak force was 100.30 N in S1–S6 and 219.40 N in S7–S10, with corresponding pull RFD values of 222.10 and 595.05 N/s. The strength measurements were obtained in specific isometric test positions and reported in absolute units. Therefore, these measurements be interpreted strictly as performance on those tests, rather than as direct measurements of propulsion during swimming or wheelchair use, or as isolated indicators of rotator cuff function. While normalizing strength to body mass is standard in non-disabled populations, such adjustments are heavily confounded in para-sport cohorts, where limb amputations, dysmelia, and severe sub-lesional muscle atrophy unevenly distort total body mass. Consequently, absolute force was retained. However, because the groups differed in age, height, body mass, and daily mobility status, and the comparisons were not adjusted for these characteristics, the independent contributions of anthropometric variance and specific impairment profiles cannot be isolated. The same caution applies to the interpretation of active ROM differences. Thus, the measured strength and ROM should be considered as task-specific group outcomes reflecting the combined functional and mobility profiles of the athletes, rather than effects attributable exclusively to functional class, evidence of shoulder injury, or the result of unmeasured cumulative exposure.

The morphological findings add to a limited para-swimming literature. In swimmers from classes S7–S10, Klich et al. described differences in supraspinatus tendon (SST) thickness and occupation ratio between distinct impairment profiles within higher sport classes (S7–S10) [12]. The present study extends these structural comparisons to athletes in a lower sport-class range. However, this comparison should not be interpreted as a continuous morphological trend across the full S1–S10 spectrum, nor as evidence of a class-specific tissue process. While greater tendon thickness and occupation ratios have also been reported in manual wheelchair users with spinal cord injuries compared to non-wheelchair controls [11], these ultrasonographic differences alone do not establish clinical tissue pathology. Furthermore, because the occupation ratio is calculated from SST thickness and AHD, it is mathematically dependent on those measurements and the specific arm position used during AHD acquisition. This complexity is reflected in the broader literature: in another cohort of para swimmers, those with chronic tendinopathy had thicker tendons yet a lower occupation ratio than asymptomatic swimmers [13]. Conversely, an observational study in wheelchair users with spinal cord injury linked a higher occupation ratio during a weight-relief raise with greater shoulder pain [19]. Given these variations across different populations and testing positions, neither greater tendon thickness nor a higher occupation ratio should be treated as a stand-alone diagnostic threshold or used to establish a clinical diagnosis in this cohort.

The higher PSFR observed in the S1–S6 group requires careful interpretation strictly within the limits of its digital processing methodology. In this study, PSFR is interpreted as a quantitative ultrasound image-texture parameter. No histological assessment was performed, and the observed difference does not establish collagen disruption, hypercel-

lularity, tendon degeneration, or a loading-related tissue response. Pozzi et al. found no significant difference in supraspinatus PSFR between participants with subacromial pain syndrome and healthy controls, and no significant association with pain, functional loss, or strength [22]. The present between-group difference therefore does not establish the diagnostic significance of PSFR. While Pożarowszczyk-Kuczko et al. [13] observed elevated PSFR in para swimmers with chronic tendinopathy compared to asymptomatic controls, divergences across studies likely stem from technical differences in ultrasound acquisition protocols, region-of-interest kernel sizing, and specific participant characteristics. Consequently, this metric should be viewed strictly as a descriptive texture feature rather than a standalone marker of tissue pathology or clinical pain.

The angle-specific reduction in AHD adds a position-dependent observation to the ultrasonographic profile. No statistically significant between-group differences were detected at 0° or 60° of shoulder abduction, whereas a statistically significant difference was observed at 90°. The mean between-group difference at 90° was 1.26 mm. Because the measurements were obtained at supported, investigator-positioned arm angles, these findings represent static, position-specific observations rather than direct assessments of dynamic scapulothoracic kinematics or humeral head translation. Furthermore, the absence of statistically significant differences at 0° and 60° should not be interpreted as evidence of equivalence between groups. Although the difference observed at 90° was statistically significant, its clinical relevance remains uncertain. AHD should therefore be interpreted alongside tendon thickness, occupation ratio, and clinical findings rather than as an independent indicator of subacromial compression or shoulder pathology [27]. Prospective studies incorporating clinical outcomes are needed to determine the functional and prognostic relevance of these observations [19].

The clinical value of the observed ultrasound profile remains uncertain. Among 80 elite wheelchair-using athletes competing in track, field, and powerlifting, Blauwet et al. found weak relationships between ultrasound-rated pathology and either shoulder pain or physical-examination findings [28]. Longitudinal MRI data from manual wheelchair users further show that structural progression and pain need not move together [29,30]. Because the present study excluded athletes with current or previous dominant-shoulder injury, impingement symptoms, or rotator cuff pathology, and did not evaluate pain or disability as outcomes, the findings cannot establish whether the observed ultrasound differences are associated with symptoms, future injury, or a need for treatment. From a methodological perspective, these findings emphasize the importance of standardized arm positioning when comparing AHD measurements across athletes and assessment sessions. Given the cross-sectional design and the absence of longitudinal clinical outcomes, the present results do not establish diagnostic thresholds, validate surveillance strategies, or support specific preventive interventions. Future prospective studies incorporating bilateral shoulder assessments, clinical outcomes, and repeated ultrasonographic measurements are needed to determine the potential clinical relevance of these observations.

Several limitations affect interpretation. The broad S1–S6 and S7–S10 categories contain heterogeneous impairment profiles, and sport class was not used as a direct measure of trunk function or lower-limb propulsion. Crucially, functional class and mobility status cannot be disentangled in the present sample. Mobility status also differed between the groups, so the present comparison cannot distinguish associations with sport class from those with wheelchair use or other participant characteristics. Consequently, the observed differences must be interpreted as associations with the athletes' combined functional and mobility profiles. The cross-sectional design precludes causal and temporal inference. Scapulothoracic kinematics, humeral head translation, and cumulative mechanical shoulder loading were not measured. The unadjusted analyses cannot separate the contributions of age, body

dimensions, impairment characteristics, and exposure. Only the dominant shoulder was assessed, and the single-session design does not establish longitudinal clinical utility.

## 5. Conclusions

In this cohort of para swimmers, athletes classified as S1–S6 exhibited lower dominant-shoulder peak force, rate of force development, and active range of motion, alongside greater supraspinatus tendon thickness, occupation ratio, and PSFR compared with athletes classified as S7–S10. Because functional class and mobility status cannot be disentangled in this sample, these differences represent associations with the athletes' combined functional and mobility profiles rather than effects attributable exclusively to functional class. The AHD was smaller in the S1–S6 group at 90° of shoulder abduction, whereas no statistically significant between-group differences were observed at 0° or 60°. Given the cross-sectional design and the absence of independent clinical assessments, these findings should be interpreted as observed functional and ultrasonographic differences rather than evidence of causal relationships, specific biomechanical mechanisms, or clinically confirmed shoulder pathology.

**Author Contributions:** Conceptualization, B.P.-K. and S.K.; methodology, B.P.-K., G.L. and S.K.; software, G.L. and S.K.; validation, B.P.-K., G.L. and S.K.; formal analysis, R.T. and M.K.; investigation, B.P.-K. and S.K.; data curation, B.P.-K. and S.K.; writing—original draft preparation, B.P.-K., G.L. and S.K.; writing—review and editing, R.T. and M.K.; visualization, G.L.; supervision, R.T., M.K., and S.K.; project administration, B.P.-K. All authors have read and agreed to the published version of the manuscript.

**Funding:** This research received no external funding.

**Institutional Review Board Statement:** The study was conducted in accordance with the Declaration of Helsinki and approved by the Senate Research Ethics Committee of Wrocław University of Health and Sport Sciences (protocol code: 07/2026; date of approval: 10 June 2026).

**Informed Consent Statement:** Informed consent was obtained from all subjects involved in the study.

**Data Availability Statement:** The data supporting the findings of this study are available from the authors upon request.

**Conflicts of Interest:** The authors declare no conflicts of interest.

## Abbreviations

The following abbreviations are used in this manuscript:

| | |
|---|---|
| AHD | Acromiohumeral Distance |
| ANOVA | Analysis of Variance |
| CI | Confidence Interval |
| df | Degrees of Freedom |
| ICC | Intraclass Correlation Coefficient |
| $MDC_{95}$ | Minimal Detectable Change at 95% Confidence Level |
| OR | Subacromial Space Occupation ratio |
| PSFR | Peak Spatial Frequency Radius |
| RFD | Rate of Force Development |
| ROM | Range of Motion |
| SD | Standard Deviation |
| SEM | Standard Error of Measurement |
| SST | Supraspinatus Tendon |

## References


1. World Para Swimming. *World Para Swimming Classification Rules and Regulations*; International Paralympic Committee: Bonn, Germany, 2022.
2. van Drongelen, S.; van der Woude, L.H.V.; Janssen, T.W.J.; Angenot, E.D.L.; Chadwick, E.K.J.; Veeger, H.E.J. Mechanical load on the upper extremity during wheelchair activities. *Arch. Phys. Med. Rehabil.* **2005**, *86*, 1214–1220. [CrossRef]
3. Collinger, J.L.; Boninger, M.L.; Koontz, A.M.; Price, R.; Sisto, S.A.; Tolerico, M.L.; Cooper, R.A. Shoulder biomechanics during the push phase of wheelchair propulsion: A multisite study of persons with paraplegia. *Arch. Phys. Med. Rehabil.* **2008**, *89*, 667–676. [CrossRef]
4. Rosa, J.; Silva, A.; Rodrigues, D.; Menslin, R.; Araújo, L.; Alves, E.; Vital, R.; Mello, M. A multi-parameter evaluation of Paralympic swimmers in the training cycle before 2016 Paralympic Games. *Hum. Mov.* **2020**, *21*, 90–99. [CrossRef]
5. Kim, S.; Park, J.; Eun, S.D.; Kang, D. The effect of pushing and pulling movements when propelling a manual wheelchair on upper limb kinematics and muscle activity in people with spinal cord injury. *Disabil. Rehabil. Assist. Technol.* **2026**, *21*, 1882–1894. [CrossRef]
6. Irmane, L.; Pontaga, I.; Upitis, I.; Solovjova, J. Swimmers' shoulder side asymmetry at rest and after aerobic load. *Hum. Mov.* **2022**, *23*, 130–139. [CrossRef]
7. Kokaly, M.; Carvallo, A.; Guzmán, C.; Prieto, M.J.; Henríquez, M.; Valencia, O. Upper-limb asymmetry in wheelchair para-athletes: A comparative analysis across sports disciplines. *Front. Sports Act. Living* **2026**, *8*, 1858941. [CrossRef]
8. Brose, S.W.; Boninger, M.L.; Fullerton, B.; McCann, T.; Collinger, J.L.; Impink, B.G.; Dyson-Hudson, T.A. Shoulder ultrasound abnormalities, physical examination findings, and pain in manual wheelchair users with spinal cord injury. *Arch. Phys. Med. Rehabil.* **2008**, *89*, 2086–2093. [CrossRef]
9. Jahanian, O.; Van Straaten, M.G.; Goodwin, B.M.; Lennon, R.J.; Barlow, J.D.; Murthy, N.S.; Morrow, M.M. Shoulder magnetic resonance imaging findings in manual wheelchair users with spinal cord injury. *J. Spinal Cord Med.* **2022**, *45*, 564–574. [CrossRef]
10. Soo Hoo, J.A.; Kim, H.; Fram, J.; Lin, Y.S.; Page, C.; Easthausen, I.; Jayabalan, P. Shoulder pain and ultrasound findings: A comparison study of wheelchair athletes, nonathletic wheelchair users, and nonwheelchair users. *PM&R* **2022**, *14*, 551–560. [CrossRef]
11. Fournier Belley, A.; Gagnon, D.H.; Routhier, F.; Roy, J.S. Ultrasonographic measures of the acromiohumeral distance and supraspinatus tendon thickness in manual wheelchair users with spinal cord injury. *Arch. Phys. Med. Rehabil.* **2017**, *98*, 517–524. [CrossRef]
12. Klich, S.; Kisilewicz, A.; Pożarowszczyk, B.; Zatoń, M.; Kawczyński, A.; Michener, L.A. Shoulder tendon characteristics in disabled swimmers in high functional classes: Preliminary report. *Phys. Ther. Sport* **2019**, *35*, 23–28. [CrossRef]
13. Pożarowszczyk-Kuczko, B.; Jabłońska, O.; Bogdański, B.; Wróblewska, Z.; Klich, S. Macro- and micro-morphological properties of the rotator cuff structures in the chronic stage of tendinopathy in Para swimmers. *J. Clin. Med.* **2026**, *15*, 2193. [CrossRef]
14. Klich, S.; Podczarska-Głowacka, M.; Valera-Calero, J.A.; Arias-Buría, J.L.; Fernández-de-Las-Peñas, C. Metrology of Supraspinatus Tendon Thickness in Swimmers with Tendinopathy Using Ultrasound Imaging: An Intra- and Inter-Rater Reliability Study. *J. Clin. Med.* **2024**, *13*, 3822. [CrossRef]
15. Collinger, J.L.; Gagnon, D.; Jacobson, J.; Impink, B.G.; Boninger, M.L. Reliability of quantitative ultrasound measures of the biceps and supraspinatus tendons. *Acad. Radiol.* **2009**, *16*, 1424–1432. [CrossRef]
16. Collings, T.J.; Goodlich, B.I.; Hams, A.H.; Bourne, M.N. Reliability of VALD DynaMo dynamometer to assess upper and lower body isometric strength in healthy adults. *Phys. Ther. Sport* **2025**, *75*, 135–143. [CrossRef]
17. Klich, S.; Madeleine, P.; Ficek, K.; Sommer, K.; Fernández-de-Las-Peñas, C.; Michener, L.A.; Kawczyński, A. Functional and morphological changes in shoulder girdle muscles after repeated climbing exercise. *Res. Sports Med.* **2023**, *31*, 787–801. [CrossRef]
18. Pożarowszczyk-Kuczko, B.; Lampart, G.; Jabłońska, O.; Podczarska-Głowacka, M.; Klich, S. Shoulder girdle muscle function and morphology after isotonic and isokinetic exercise in swimmers with rotator cuff tendinopathy. *Res. Sports Med.* **2026**, 1–12. [CrossRef]
19. Eyvaz, N.; Adar, S.; Akçin, A.İ.; Doğanlar, N.; Dündar, Ü.; Toktaş, H.; Yeşil, H.; Eroğlu, S.; Beştaş, E. Shoulder Structural Changes in Manual Wheelchair Users with Spinal Cord Injury: Cross-Sectional Ultrasound Study of Supraspinatus Tendon Thickness and Acromiohumeral Distance. *Arch. Phys. Med. Rehabil.* **2026**, *107*, 1950–1957. [CrossRef]
20. von Elm, E.; Altman, D.G.; Egger, M.; Pocock, S.J.; Gøtzsche, P.C.; Vandenbroucke, J.P.; STROBE Initiative. Strengthening the Reporting of Observational Studies in Epidemiology (STROBE) statement: Guidelines for reporting observational studies. *BMJ* **2007**, *335*, 806–808. [CrossRef]
21. Ahmadi, S.; Uchida, M.C. Place of the gold standard isokinetic dynamometer in Paralympic sports: A systematic review. *Hum. Mov.* **2021**, *22*, 1–10. [CrossRef]
22. Pozzi, F.; Seitz, A.L.; Plummer, H.A.; Chow, K.; Bashford, G.R.; Michener, L.A. Supraspinatus tendon micromorphology in individuals with subacromial pain syndrome. *J. Hand Ther.* **2017**, *30*, 214–220. [CrossRef]

23. Vila-Dieguez, O.; Heindel, M.D.; Zipser, M.C.; Mortazavi, K.; Kulig, K.; Bashford, G.; Mack, W.; Michener, L.A. Relationship Between Tendon Tissue and Shoulder Disability Change During an 8-Week Exercise Intervention for Rotator Cuff Tendinopathy: An Observational Study. *Phys. Ther.* **2025**, *105*, pzaf107. [CrossRef]
24. Bashford, G.R.; Tomsen, N.; Arya, S.; Burnfield, J.M.; Kulig, K. Tendinopathy discrimination by use of spatial frequency parameters in ultrasound B-mode images. *IEEE Trans. Med. Imaging* **2008**, *27*, 608–615. [CrossRef]
25. Pearson, S.J.; Engel, A.J.; Bashford, G.R. Changes in tendon spatial frequency parameters with loading. *J. Biomech.* **2017**, *57*, 136–140. [CrossRef]
26. Lin, Y.-S.; Boninger, M.L.; Day, K.A.; Koontz, A.M. Ultrasonographic measurement of the acromiohumeral distance in spinal cord injury: Reliability and effects of shoulder positioning. *J. Spinal Cord Med.* **2015**, *38*, 700–708. [CrossRef]
27. Mozingo, J.D.; Akbari-Shandiz, M.; Van Straaten, M.G.; Murthy, N.S.; Schueler, B.A.; Holmes, D.R., 3rd; McCollough, C.H.; Zhao, K.D. Comparison of glenohumeral joint kinematics between manual wheelchair tasks and implications on the subacromial space: A biplane fluoroscopy study. *J. Electromyogr. Kinesiol.* **2022**, *62*, 102350. [CrossRef]
28. Blauwet, C.A.; Chakraverty, J.; Derman, W.; Idrisova, G.; Martin, P.; Miller, S.C.; Morrissey, D.; Webborn, N. Shoulder Pain, Function, and Ultrasound-Determined Structure in Elite Wheelchair-Using Para Athletes: An Observational Study. *Med. Sci. Sports Exerc.* **2022**, *54*, 896–904. [CrossRef]
29. Jahanian, O.; Van Straaten, M.G.; Barlow, J.D.; Murthy, N.S.; Morrow, M.M.B. Progression of rotator cuff tendon pathology in manual wheelchair users with spinal cord injury: A 1-year longitudinal study. *J. Spinal Cord Med.* **2023**, *46*, 466–476. [CrossRef]
30. Arnet, U.; Veeger, D.H.E.J.; de Vries, W.H.K. Shoulder load during wheelchair-related activities of daily life. *J. Electromyogr. Kinesiol.* **2025**, *84*, 103027. [CrossRef]


**Disclaimer/Publisher's Note:** The statements, opinions and data contained in all publications are solely those of the individual author(s) and contributor(s) and not of MDPI and/or the editor(s). MDPI and/or the editor(s) disclaim responsibility for any injury to people or property resulting from any ideas, methods, instructions or products referred to in the content.